JOURNAL OF GUIDANCE, CONTROL, AND DYNAMICS
Vol. 28, No. 6, November–December 2005

Analytical Solutions for Thrusting, Spinning Spacecraft Subject to Constant Forces

James M. Longuski*
Purdue University, West Lafayette, Indiana 47907-2023
R. Anne Gick†
The Aerospace Corporation, Chantilly, Virginia 20151
Mohammad A. Ayoubi‡
Purdue University, West Lafayette, Indiana 47907-2023
and
Laura Randall§
Space Systems/Loral, Palo Alto, California 94303-4604

A spinning, nearly axisymmetric rigid body is subject to constant, body-fixed forces and transverse body-fixed torques. Because no torque is applied along the spin axis and the rigid body is nearly axisymmetric, the spin rate remains nearly constant. By further assuming small angular excursions of the spin axis (with respect to an inertially fixed direction), approximate closed-form analytical solutions are obtained for attitude, rotational, and translational motion. The compact solutions in complex form are eminently suitable for analyzing maneuvers of spinning spacecraft. Numerical simulations confirm that the solutions are highly accurate when applied to typical motion of a spacecraft such as the Galileo spacecraft.

Nomenclature

A	=	transformation matrix relating body and inertial frames
c	=	cosine
F	=	rescaled transverse body-fixed torque, $1/s^2$
f	=	body-fixed force, N
H	=	angular momentum in inertial frame, $kg \cdot m^2/s$
h	=	angular momentum in body-fixed frame, $kg \cdot m^2/s$
I	=	moment of inertia, $kg \cdot m^2$
M	=	body-fixed moment, $N \cdot m$
s	=	sine
v	=	inertial velocity, m/s
ΔV	=	change in inertial velocity, m/s
ρ	=	pointing error, rad
ϕ	=	Euler angle, rad
ω	=	angular velocity, rad/s

Subscripts

a	=	axial
ad	=	axial inertial displacement
av	=	axial inertial velocity
sec	=	secular term
t	=	transverse
td	=	transverse inertial displacement
tv	=	transverse inertial velocity
X, Y, Z	=	components in inertial frame
x, y, z	=	components in body-fixed frame

Superscript

$*$	=	complex conjugate

Introduction

In the past few decades analytical solutions have been developed for satellite attitude computations, significantly extending the classical torque-free and rigid-body assumptions of Poinsot motion.[1–5] New formulations for Poinsot motion have also been presented.[6,7] The problem of the motion of spinning (and dual-spin) spacecraft presents many interesting challenges in stability and control, maneuver optimization, and nonlinear dynamics.[8–11]

In an effort to achieve insight into the behavior of spinning spacecraft, numerous investigators have sought closed-form analytical solutions. Such closed-form solutions prove to be extremely useful in parametric studies, error analyses, onboard computations, optimal control, and stability analyses. In the work by Larson and Likins,[12] a closed-form solution is obtained for linearized equations in which transverse torques are present and the spin rate is constant. Cochran and Shu[13] provide an exact solution for the free motion of a dual-spin spacecraft.

A solution is given by Bödewadt[14] and discussed by Leimanis[15] for the axisymmetric rigid body subject to body-fixed torques about its principal axes. However, as pointed out and explained by Longuski,[16] the solution for the orientation of the body in inertial space is incorrect in these references. Longuski deals with the nearly axisymmetric[17,18] case and includes analytical solutions for the Eulerian velocities (which reduces to the exact solution of Bödewadt in the axisymmetric case) and approximate analytical solutions for the Eulerian angles that provide the orientation of the body in inertial space. The accuracy of these solutions is tested and reported on by Longuski et al.[19] Using Longuski's solution as a first-order approximation, Price[20] develops a semianalytic solution in the form of a power series in one of the applied torques. Although the series converges rapidly, the method is limited to selected time intervals, having short-term validity. Van der Ha[21] presents a perturbation solution for the attitude motion subject to constant body-fixed torques, based on the ratio of transverse-to-spin-rotation rate as the

Received 16 July 2004; revision received 3 December 2004; accepted for publication 7 December 2004.

*Professor, School of Aeronautics and Astronautics, 315 N. Grant Street; longuski@ecn.purdue.edu. Associate Fellow AIAA.

†Senior Engineering Specialist, 15049 Conference Center Drive; RAnne.Gick@aero.org.

‡Ph.D. Candidate, School of Aeronautics and Astronautics; maayoubi@purdue.edu.

§Systems Engineer, M/S G19, 3825 Fabian Way; randall.laura@ssd.loral.com.

small parameter, but this solution is also valid only for short time intervals.

The problem of a spinning, thrusting rigid body is important in astrodynamics because it has applications in the maneuver analysis of rockets and spacecraft. Early in the development of rocket flight, some theoretical analyses on spin-stabilized rockets appeared, most notably, those by Rosser et al.[22] and Davis et al.[23] Later, with the development of lunar and interplanetary spacecraft, interest in analytical solutions for the motion of a thrusting, spinning rigid body was reawakened. Such analyses can provide important insight into the errors occurring during axially thrusting and spinning-up spacecraft maneuvers. Theoretical models for the axisymmetric case are skillfully presented by Armstrong,[24] who cites Refs. 22 and 23 as classic, original works on the subject.

The problem of error analysis of spacecraft ΔV maneuvers has become important in the assessment of more complex spacecraft such as the Galileo, which is a dual-spinner (for example, see Longuski[25] and Longuski et al.[26]). The analytical problems presented by this spacecraft have provided new challenges and a source of inspiration in the development of more general theories. Even in the case where the Galileo performs maneuvers in all-spin mode (and hence can be treated as a single spinner), it poses difficulties because the spacecraft is not quite axisymmetric, and it is necessary to account for the small asymmetry. Tsiotras and Longuski[27] provide analytical solutions for the attitude dynamics of a nearly axisymmetric rigid body, subject to constant body-fixed torques about three axes. These solutions can be used to analyze the spin-up maneuver of the Galileo in which a single thruster creates a large torque about the spin axis, but also creates significant torques about the transverse axes. (Thruster couples, which could cancel transverse torques, could not be used on the Galileo spacecraft because of overriding concerns about plume impingement on sensitive scientific instruments.) In addition, Klumpe and Longuski[28] and Beck and Longuski[29] present some results for the velocity accumulated during three-axis torquing caused by constant body-fixed forces along all three axes.

In this paper, we look at the thrusting, spinning spacecraft problem. The spin rate and body-fixed forces are assumed constant. We find that using complex variables contributes significantly to the compactness of the final solutions. The advantage of the complex formulation has been noted by Leimanis,[15] Armstrong,[24] Tsiotras and Longuski,[27] and Randall et al.[30] We present approximate closed-form solutions for attitude motion. Also, because displacement can be important in operations near a shuttle or a space station and in the case of formation flying, closed-form solutions are given for translational motion. Closed-form solutions are given for angular velocities, Eulerian angles, angular momentum, transverse velocities, transverse displacement, axial velocity, and axial displacement. The results are valid for axisymmetric and nearly axisymmetric bodies.

Closed-Form Solutions for Angular Velocities

The rotational motion of a rigid body in the body-fixed coordinate system is governed by Euler's equations of motion,[31] which for principal axes, can be written as

$$\dot{\omega}_x = M_x/I_x - [(I_z - I_y)/I_x]\omega_y\omega_z \tag{1}$$

$$\dot{\omega}_y = M_y/I_y - [(I_x - I_z)/I_y]\omega_z\omega_x \tag{2}$$

$$\dot{\omega}_z = M_z/I_z - [(I_y - I_x)/I_z]\omega_x\omega_y \tag{3}$$

We assume that the body is spinning about its z axis and there is no axial torque ($M_z = 0$). (We note that in practice there might be a small component of axial torque from thruster misalignment or from swirl torque; in many cases this small component can be ignored, and the following analysis applies.) For an axisymmetric body ($I_x = I_y$), nearly axisymmetric body ($I_x \approx I_y$), or when $\omega_x\omega_y$ is negligible even when the body is asymmetric ($\omega_x\omega_y \approx 0$), Eq. (3) integrates to

$$\omega_z \approx \omega_{z0} = \omega_z(0) \tag{4}$$

which is, of course, exact for an axisymmetric body. (In applications, most spinning spacecraft will in fact be nearly axisymmetric rather than exactly axisymmetric.) By defining new variables as

$$\Omega_x \equiv \omega_x\sqrt{k_y}, \qquad \Omega_y \equiv \omega_y\sqrt{k_x} \tag{5}$$

$$k_x \equiv (I_z - I_y)/I_x, \qquad k_y \equiv (I_z - I_x)/I_y \tag{6}$$

$$k \equiv \sqrt{k_x k_y} \tag{7}$$

we can combine Eqs. (1) and (2) into the following linear, first-order scalar, but complex differential equation:

$$\dot{\Omega} - ik\omega_{z0}\Omega = F \tag{8}$$

where

$$\Omega \equiv \Omega_x + i\Omega_y \tag{9}$$

$$F \equiv F_x + iF_y \tag{10}$$

$$F_x \equiv (M_x/I_x)\sqrt{k_y}, \qquad F_y \equiv (M_y/I_y)\sqrt{k_x} \tag{11}$$

The solution to Eq. (8) can be written compactly as follows:

$$\Omega(t) = \Omega_0 e^{ik\omega_{z0}t} + (iF/k\omega_{z0})(1 - e^{ik\omega_{z0}t}), \qquad \Omega_0 = \Omega(0) \tag{12}$$

The first term on the right-hand side of Eq. (12) is the solution caused by the initial conditions, also called the homogeneous solution. The second term describes the response from the forcing function F, also called the nonhomogeneous solution. The solution for the transverse angular velocities is as follows:

$$\omega_x = \frac{\mathrm{Re}[\Omega(t)]}{\sqrt{k_y}} = \frac{\Omega(t) + \Omega^*(t)}{2\sqrt{k_y}} \tag{13}$$

$$\omega_y = \frac{\mathrm{Im}[\Omega(t)]}{\sqrt{k_x}} = \frac{\Omega(t) - \Omega^*(t)}{2i\sqrt{k_x}} \tag{14}$$

where Re and Im indicate the real and imaginary parts, respectively, and where the asterisk denotes the complex conjugate.

Closed-Form Solutions for Eulerian Angles

We use a 3-1-2 Euler angle sequence[32] to describe the orientation of the body-fixed reference frame with respect to an inertially fixed reference frame. The corresponding kinematic equations are

$$\dot{\phi}_x = \omega_x\cos\phi_y + \omega_z\sin\phi_y \tag{15}$$

$$\dot{\phi}_y = \omega_y - (\omega_z\cos\phi_y - \omega_x\sin\phi_y)\tan\phi_x \tag{16}$$

$$\dot{\phi}_z = (\omega_z\cos\phi_y - \omega_x\sin\phi_y)\sec\phi_x \tag{17}$$

These equations are highly nonlinear and seemingly intractable, although much progress has been made using linearization, for example, by assuming ϕ_x and ϕ_y are small.[18] Using small-angle approximations for ϕ_x and ϕ_y and a further assumption that $\phi_y\omega_x$ is small compared to ω_z reduces Eqs. (15–17) to

$$\dot{\phi}_x \approx \omega_x + \phi_y\omega_z \tag{18}$$

$$\dot{\phi}_y \approx \omega_y - \phi_x\omega_z \tag{19}$$

$$\dot{\phi}_z \approx \omega_z \tag{20}$$

The solution to Eq. (20) is simply

$$\phi_z(t) = \omega_{z0}t + \phi_{z0}, \qquad \phi_{z0} = \phi_z(0) \tag{21}$$

Combining Eqs. (18) and (19) provides

$$\dot{\phi} + i\omega_{z0}\phi = \omega \tag{22}$$

where the complex variables ϕ and ω are defined as

$$\phi \equiv \phi_x + i\phi_y \tag{23}$$

$$\omega \equiv \omega_x + i\omega_y \tag{24}$$

Equation (22) has the following solution:

$$\phi(t) = \phi_0 e^{-i\omega_{z0}t} + e^{-i\omega_{z0}t} I_\phi(t), \qquad \phi_0 = \phi(0) \tag{25}$$

The nonhomogeneous solution involves $I_\phi(t)$, which is defined as

$$I_\phi(t) \equiv \int_0^t e^{i\omega_{z0}\tau}\omega(\tau)\,\mathrm{d}\tau \tag{26}$$

Therefore, to solve for the Eulerian angles, we need to evaluate $I_\phi(t)$. By using Eqs (5), (6), (9), and (24), we note that $\omega(t)$ can be expressed in terms of $\Omega(t)$ as follows:

$$\omega(t) = k_1\Omega(t) + k_2\Omega^*(t) \tag{27}$$

where k_1 and k_2 are defined as

$$k_1 \equiv \left(\sqrt{k_x} + \sqrt{k_y}\right)\Big/2k, \qquad k_2 \equiv \left(\sqrt{k_x} - \sqrt{k_y}\right)\Big/2k \tag{28}$$

and $I_\phi(t)$ is given by

$$I_\phi(t) = k_1 I_{\phi 1}(t) + k_2 I_{\phi 2}(t) \tag{29}$$

in which

$$\begin{aligned} I_{\phi 1}(t) &= \int_0^t e^{i\omega_{z0}\tau}\Omega(\tau)\,\mathrm{d}\tau \\ &= \frac{-i\Omega_0}{\mu\omega_{z0}}(e^{i\mu\omega_{z0}t} - 1) + \frac{F}{k\omega_{z0}^2}\left[(e^{i\omega_{z0}t} - 1) - \frac{1}{\mu}(e^{i\mu\omega_{z0}t} - 1)\right] \end{aligned} \tag{30}$$

$$\begin{aligned} I_{\phi 2}(t) &= \int_0^t e^{i\omega_{z0}\tau}\Omega^*(\tau)\,\mathrm{d}\tau \\ &= \frac{-i\Omega_0^*}{\kappa\omega_{z0}}(e^{i\kappa\omega_{z0}t} - 1) - \frac{F^*}{k\omega_{z0}^2}\left[(e^{i\omega_{z0}t} - 1) - \frac{1}{\kappa}(e^{i\kappa\omega_{z0}t} - 1)\right] \end{aligned} \tag{31}$$

where

$$\mu \equiv 1 + k, \qquad \kappa \equiv 1 - k \tag{32}$$

Thus the solutions for the Eulerian angles are known explicitly in terms of circular functions. These circular functions remain bounded as functions of time so that the nutation will remain bounded.

Closed-Form Solutions for Angular Momentum

The inertial and body components of angular momentum vector are related by the following equation:

$$\begin{Bmatrix} H_X \\ H_Y \\ H_Z \end{Bmatrix} = [A] \begin{Bmatrix} h_x \\ h_y \\ h_z \end{Bmatrix} \tag{33}$$

where

$$h_x = I_x\omega_x \tag{34}$$

$$h_y = I_y\omega_y \tag{35}$$

$$h_z = I_z\omega_z \tag{36}$$

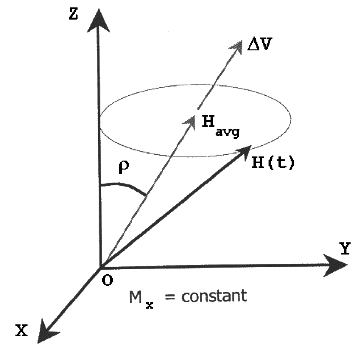

Fig. 1 Motion of angular momentum vector in inertial space (based on Ref. 34).

and the direction cosine matrix $[A]$, corresponding to a 3-1-2 Euler angle sequence,[32] is given by

$$[A] = \begin{bmatrix} c\phi_z c\phi_y - s\phi_z s\phi_x s\phi_y & -s\phi_z c\phi_x & c\phi_z s\phi_y + s\phi_z s\phi_x c\phi_y \\ s\phi_z c\phi_y + c\phi_z s\phi_x s\phi_y & c\phi_z c\phi_x & s\phi_z s\phi_y - c\phi_z s\phi_x c\phi_y \\ -c\phi_x s\phi_y & s\phi_x & c\phi_x c\phi_y \end{bmatrix} \tag{37}$$

where c and s indicate cosine and sine, respectively. From Eqs. (33) and (37), the transverse angular momentum vector can be written in complex form as

$$H = e^{i\phi_z}[h_x(c\phi_y + is\phi_x s\phi_y) + h_y(ic\phi_x) + h_z(s\phi_y - is\phi_x c\phi_y)] \tag{38}$$

Now, by defining

$$H \equiv H_X + iH_Y \tag{39}$$

$$h \equiv h_x + ih_y \tag{40}$$

and with the assumptions that ϕ_x and ϕ_y are small and that the product $\phi_x\phi_y$ is negligible, then a useful approximation is obtained for the angular momentum:

$$H \approx (h - ih_z\phi)e^{i\phi_z} \tag{41}$$

We use two methods to simplify Eq. (41). In the first method, Eqs. (21), (25), and (34–36) are substituted into Eq. (41), and after lengthy algebraic manipulations and simplification we get

$$H = (iM/\omega_{z0})(1 - e^{i\omega_{z0}t}) \tag{42}$$

where

$$M \equiv M_x + iM_y \tag{43}$$

Equation (42) is an equation of a circle in the inertial plane (H_X, H_Y) with a center at $(-M_y/\omega_{z0}, M_x/\omega_{z0})$ and a radius $\sqrt{(M_x^2 + M_y^2)}/\omega_{z0}$. This behavior is illustrated in Fig. 1, where we show the case when $M_x \neq 0$ and $M_y = 0$. The H vector describes small circle in inertial space where the center of circle represents the average position of angular momentum, which has nonzero components along the inertial X and Y and no component along inertial X axis. The average pointing error ρ of the angular momentum vector with respect to inertial Z axis is $\sqrt{(M_x^2 + M_y^2)}/(I_z\omega_{z0}^2)$ assuming $\rho \ll 1$ rad. For the second method, we refer the interested reader to Gick's Ph.D. dissertation.[33] Longuski et al.[19] also describe this behavior in an earlier work.

Closed-Form Solutions for Transverse Velocities

In the analysis that follows we assume that the force components f_x, f_y, and f_z remain constant. The inertial and body components of acceleration are related by the following equation:

$$\begin{Bmatrix} \dot{v}_X \\ \dot{v}_Y \\ \dot{v}_Z \end{Bmatrix} = [A] \begin{Bmatrix} f_x/m \\ f_y/m \\ f_z/m \end{Bmatrix} \tag{44}$$

When ϕ_x and ϕ_y are small, Eq. (37) becomes

$$[A] \approx \begin{bmatrix} c\phi_z & -s\phi_z & \phi_y c\phi_z + \phi_x s\phi_z \\ s\phi_z & c\phi_z & \phi_y s\phi_z - \phi_x c\phi_z \\ -\phi_y & \phi_x & 1 \end{bmatrix} \tag{45}$$

By introducing the complex functions

$$v \equiv v_x + i v_y \tag{46}$$

$$f \equiv f_x + i f_y \tag{47}$$

and using Eq. (23), we can write Eq. (44) as follows for the transverse and axial acceleration in the inertial frame:

$$\dot{v} = e^{i\phi_z}(f - i f_z \phi)\big/m \tag{48}$$

$$\dot{v}_Z = \left[f_z + (i/2)(f^*\phi - f\phi^*)\right]\big/m \tag{49}$$

where v_Z is real. (We solve for v_Z in a later section.) By integrating the transverse acceleration, Eq. (48), we get

$$v(t) = \left(\frac{f}{m}\right)\int_0^t e^{i\phi_z(\tau)}\,\mathrm{d}\tau - \left(\frac{i f_z}{m}\right)\int_0^t e^{i\phi_z(\tau)}\phi(\tau)\,\mathrm{d}\tau \tag{50}$$

Substituting the expressions for ϕ_z and ϕ, Eqs. (21) and (25), respectively, into the Eq. (50) provides

$$v(t) = v(0) + i e^{i\varphi_{z0}}\left\{(f/\omega_{z0})(1 - e^{i\omega_{z0}t}) - f_z[\varphi_0 t + I_{\mathrm{tv}}(t)]\right\}\big/m \tag{51}$$

where

$$I_{\mathrm{tv}}(t) = k_1 I_{\mathrm{tv}1}(t) + k_2 I_{\mathrm{tv}2}(t) \tag{52}$$

$$I_{\mathrm{tv}1}(t) = \left(iF\big/k\omega_{z0}^3\right)(1 - e^{i\omega_{z0}t}) - \left(i\big/\mu^2\omega_{z0}^2\right)(i\Omega_0 + F/k\omega_{z0}) \times (1 - e^{i\mu\omega_{z0}t}) + (1/\mu\omega_{z0})(i\Omega_0 - F/\omega_{z0})t \tag{53}$$

$$I_{\mathrm{tv}2}(t) = \left(-iF^*\big/k\omega_{z0}^3\right)(1 - e^{i\omega_{z0}t}) - \left(i\big/\kappa^2\omega_{z0}^2\right)\left(i\Omega_0^* - F^*\big/k\omega_{z0}\right) \times (1 - e^{i\kappa\omega_{z0}t}) + (1/\kappa\omega_{z0})\left(i\Omega_0^* - F^*\big/\omega_{z0}\right)t \tag{54}$$

We note in Eqs. (53) and (54) the appearance of secular terms (i.e., terms that grow monotonically with time). As expected, the axial component of velocity v_Z must grow linearly with time, and therefore it is not surprising that the transverse components also exhibit secular effects. We will discuss this behavior further in the axial-velocity section.

Closed-Form Solutions for Transverse Displacements

Because the analysis of position in space could have important applications in spacecraft maneuvers near other spacecraft (i.e., formation flying) or in the vicinity of a space station or a shuttle, we present here some closed-form solutions for transverse and axial displacements. Transverse displacements can be found by integrating Eq. (51):

$$d(t) = d(0) + \int_0^t v(\tau)\,\mathrm{d}\tau = d(0) + \int_0^t v_X(\tau)\,\mathrm{d}\tau + i\int_0^t v_Y(\tau)\,\mathrm{d}\tau \tag{55}$$

where

$$d \equiv d_X + i d_Y \tag{56}$$

After some algebraic simplification, we obtain

$$d(t) = d(0) - \frac{f e^{i\varphi_{z0}}}{m\omega_{z0}^2}(1 - e^{i\omega_{z0}t}) + \left[v(0) + \frac{if}{m\omega_{z0}}e^{i\varphi_{z0}}\right]t - \frac{i f_z \varphi_0}{m}e^{i\varphi_{z0}}t^2 - \frac{i f_z}{m}e^{i\varphi_{z0}}I_{\mathrm{td}}(t) \tag{57}$$

where

$$I_{\mathrm{td}}(t) = k_1 I_{\mathrm{td}1}(t) + k_2 I_{\mathrm{td}2}(t) \tag{58}$$

$$I_{\mathrm{td}1}(t) = \int_0^t I_{\mathrm{tv}1}(\tau)\,\mathrm{d}\tau = \frac{F}{k\omega_{z0}^4}(1 - e^{i\omega_{z0}t}) - \frac{1}{\mu^3\omega_{z0}^3}\left(i\Omega_0 + \frac{F}{k\omega_{z0}}\right)(1 - e^{i\mu\omega_{z0}t}) - \frac{i}{\mu^2\omega_{z0}^2}\left[i\Omega_0 - \frac{(\mu^2-1)F}{k\omega_{z0}}\right]t + \frac{1}{2\mu\omega_{z0}}\left(i\Omega_0 - \frac{F}{\omega_{z0}}\right)t^2 \tag{59}$$

$$I_{\mathrm{td}2}(t) = \int_0^t I_{\mathrm{tv}2}(\tau)\,\mathrm{d}\tau = \frac{-F^*}{k\omega_{z0}^4}(1 - e^{i\omega_{z0}t}) - \frac{1}{\kappa^3\omega_{z0}^3}\left(i\Omega_0^* - \frac{F^*}{k\omega_{z0}}\right)(1 - e^{i\kappa\omega_{z0}t}) - \frac{i}{\kappa^2\omega_{z0}^2}\left[i\Omega_0^* + \frac{(\kappa^2-1)F^*}{k\omega_{z0}}\right]t + \frac{1}{2\kappa\omega_{z0}}\left(i\Omega_0^* - \frac{F^*}{\omega_{z0}}\right)t^2 \tag{60}$$

Closed-Form Solution for Axial Velocity

The solution for the axial velocity is found by integrating of the axial acceleration, Eq. (49), as follows:

$$v_Z(t) = v_Z(0) + \frac{f_z}{m}t + \frac{i}{2m}\left[f^*\int_0^t \varphi(\tau)\,\mathrm{d}\tau - f\int_0^t \varphi^*(\tau)\,\mathrm{d}\tau\right] \tag{61}$$

where

$$\int_0^t \varphi(\tau)\mathrm{d}\tau = -\frac{i\varphi_0}{\omega_{z0}}(1 - e^{-i\omega_{z0}t}) + I_{\mathrm{av}}(t) \tag{62}$$

$$I_{\mathrm{av}}(t) = k_1 I_{\mathrm{av}1}(t) + k_2 I_{\mathrm{av}2}(t) \tag{63}$$

$$I_{\mathrm{av}1}(t) = \frac{iF}{k\omega_{z0}^3}(1 - e^{-i\omega_{z0}t}) + \frac{F}{k\omega_{z0}^2}t - \frac{i}{k\mu\omega_{z0}^2}\left(i\Omega_0 + \frac{F}{k\omega_{z0}}\right)(\mu - e^{ik\omega_{z0}t} - ke^{-i\omega_{z0}t}) \tag{64}$$

$$I_{\mathrm{av}2}(t) = \frac{-iF^*}{k\omega_{z0}^3}(1 - e^{-i\omega_{z0}t}) - \frac{F^*}{k\omega_{z0}^2}t + \frac{i}{k\kappa\omega_{z0}^2}\left(i\Omega_0^* - \frac{F^*}{k\omega_{z0}}\right)(\kappa - e^{-ik\omega_{z0}t} + ke^{-i\omega_{z0}t}) \tag{65}$$

In Eq. (61) we see the expected term $f_z t/m$, which for nonzero f_z represents the dominant effect. Let us now consider the important effect of the secular terms in the transverse and axial-velocity solutions. By using Eqs. (51–54), (61), and (63–65) and setting all of the initial conditions to zero, we can show that as $t \to \infty$ the velocity ratio (which only depends on the secular terms) can be found from the following equation:

$$v_{\mathrm{sec}}/v_{Z\,\mathrm{sec}} = v_{X\,\mathrm{sec}}/v_{Z\,\mathrm{sec}} + i(v_{Y\,\mathrm{sec}}/v_{Z\,\mathrm{sec}}) \tag{66}$$

where

$$\frac{v_{X\,\mathrm{sec}}}{v_{Z\,\mathrm{sec}}} = \frac{-M_y \big/ I_z\omega_{z0}^2}{1 + M_x(f_y/f_z)\big/k_x I_x\omega_{z0}^2 - M_y(f_x/f_z)\big/k_y I_y\omega_{z0}^2} \tag{67}$$

$$\frac{v_{Y\,\mathrm{sec}}}{v_{Z\,\mathrm{sec}}} = \frac{M_x \big/ I_z\omega_{z0}^2}{1 + M_x(f_y/f_z)\big/k_x I_x\omega_{z0}^2 - M_y(f_x/f_z)\big/k_y I_y\omega_{z0}^2} \tag{68}$$

We note that when there are no transverse forces (i.e., when $f_x = f_y = 0$) the velocity is aligned with the average angular momentum vector as illustrated in Fig. 1. When transverse torque is not present (i.e., $F = 0$, $M_x = M_y = 0$), then the velocity pointing error [given by Eqs. (67) and (68)] approaches zero as time goes to infinity. However, in practice transverse torques usually arise from center-of-mass offset and misalignment of axial thruster.

Closed-Form Solution for Axial Displacement

Similar to the case of transverse displacements, the axial displacement can be found by integrating Eq. (49):

$$d_Z(t) = d_Z(0) + \int_0^t v_Z(\tau)\,\mathrm{d}\tau \tag{69}$$

After some algebra, we find

$$d_Z(t) = d_Z(0) + v_Z(0)t + (f_z/2m)t^2 + (i/2m)\left[f^* I_a(t) - f I_a^*(t)\right] \tag{70}$$

where

$$\begin{aligned} I_a(t) &= \int_0^t \left[\left(\frac{-i\varphi_0}{\omega_{z0}}\right)\left(1 - e^{-i\omega_z\tau}\right) + I_{\mathrm{av}}(\tau)\right]\mathrm{d}\tau \\ &= \left(\frac{-i\varphi_0}{\omega_{z0}}\right)\left[\left(\frac{i}{\omega_{z0}}\right)(1 - e^{-i\omega_z t}) + t\right] + k_1 I_{\mathrm{ad1}}(t) + k_2 I_{\mathrm{ad2}}(t) \end{aligned} \tag{71}$$

$$\begin{aligned} I_{\mathrm{ad1}}(t) = {}& \frac{1}{\mu\omega_{z0}^3}\left(i\Omega_0 - \frac{F}{\omega_{z0}}\right)(1 - e^{-i\omega_{z0}t}) \\ & - \frac{1}{k^2\mu\omega_{z0}^3}\left(i\Omega_0 + \frac{F}{k\omega_{z0}}\right)(1 - e^{ik\omega_{z0}t}) \\ & - \frac{i}{k\omega_{z0}^2}\left(i\Omega_0 + \frac{\kappa F}{k\omega_{z0}}\right)t + \frac{Ft^2}{2k\omega_{z0}^2} \end{aligned} \tag{72}$$

$$\begin{aligned} I_{\mathrm{ad2}}(t) = {}& \frac{1}{\kappa\omega_{z0}^3}\left(i\Omega_0^* - \frac{F^*}{\omega_{z0}}\right)(1 - e^{-i\omega_{z0}t}) \\ & - \frac{1}{k^2\kappa\omega_{z0}^3}\left(i\Omega_0^* - \frac{F^*}{k\omega_{z0}}\right)(1 - e^{-ik\omega_{z0}t}) \\ & + \frac{i}{k\omega_{z0}^2}\left(i\Omega_0^* - \frac{\mu F^*}{k\omega_{z0}}\right)t - \frac{F^*t^2}{2k\omega_{z0}^2} \end{aligned} \tag{73}$$

As we expect, because Eqs. (72) and (73) are obtained by integration of Eqs. (64) and (65) respectively, (linear and parabolic) secular terms appear in the axial displacement.

Simulation and Numerical Results

We simulate the motion of the Galileo spacecraft[19] to compare our analytical solutions with the exact solutions. By "exact solutions," we mean a highly precise numerical integration of Eqs. (1–3) and (15–17). Of course we use Eq. (33) to obtain the angular momentum vector in inertial space. To obtain the exact displacement, we first numerically integrate Eq. (44) using Eq. (37) for the direction cosine matrix, and then we numerically integrate the resulting exact velocities. We use a Runge–Kutta, fourth-order, double-precision numerical integration with a tolerance of 10^{-18} to obtain our so-called exact solution. Because the errors in the analytical solution are several orders of magnitude greater than those in our exact solution, the difference provides the error in the analytical solution to the precision indicated in the plots that follow. The thrusting maneuver is assumed to last for 60 s with the following mass properties and initial conditions:

$$\begin{gathered} m = 2000\ \mathrm{kg}, \qquad I_x = 3012\ \mathrm{kg\cdot m^2} \\ I_y = 2761\ \mathrm{kg\cdot m^2}, \qquad I_z = 4627\ \mathrm{kg\cdot m^2} \end{gathered} \tag{74}$$

$$v_X(0) = v_Y(0) = v_Z(0) = d_X(0) = d_Y(0) = d_Z(0) = 0 \tag{75}$$

$$\begin{gathered} \phi_x(0) = \phi_y(0) = \phi_z(0) = \omega_x(0) = \omega_y(0) = 0 \\ \omega_z(0) = 10\ \mathrm{rpm} \end{gathered} \tag{76}$$

$$f_x = f_y = M_y = M_z = 0, \qquad f_z = 400\ \mathrm{N}, \qquad M_x = 8\ \mathrm{N\cdot m} \tag{77}$$

The 400-N engine is aligned with the spin axis (the z axis) but has a 0.02-m center-of-mass offset along the x axis so that $M_x = 8\ \mathrm{N\cdot m}$.

We select this case because it illustrates several important features of the analytical solution particularly concerning the velocity components. (Nonzero values for f_x and f_y have bounded effects on the transverse velocity even when the axial force and transverse torques are nonzero, and so we do not present numerical results for these cases.)

In Fig. 2, we show the exact solution (indicated by a solid line) for $\omega_x(t)$ and the analytical solution (represented by a dashed line) for $\omega_x(t)$, obtained from Eq. (13). The difference between these solutions is indistinguishable in the plot. To display the error in the analytical solution, we plot the difference between the solutions (i.e., the exact minus analytical) in Fig. 3. Here we see that, although

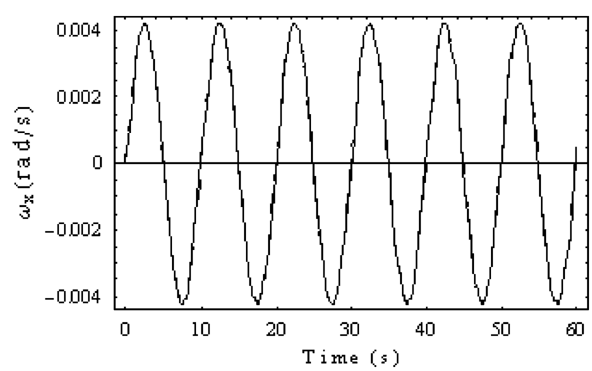

Fig. 2 Exact and analytical and solutions for angular velocity ω_x.

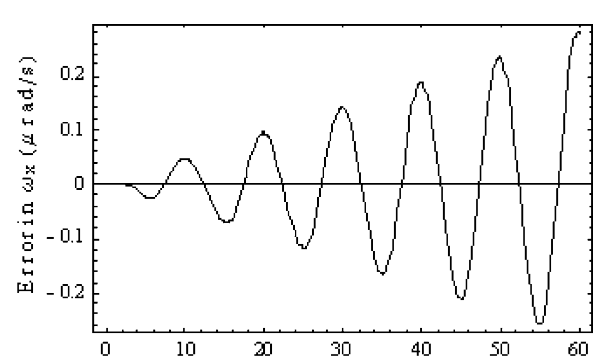

Fig. 3 Exact minus analytical solution of angular velocity ω_x.

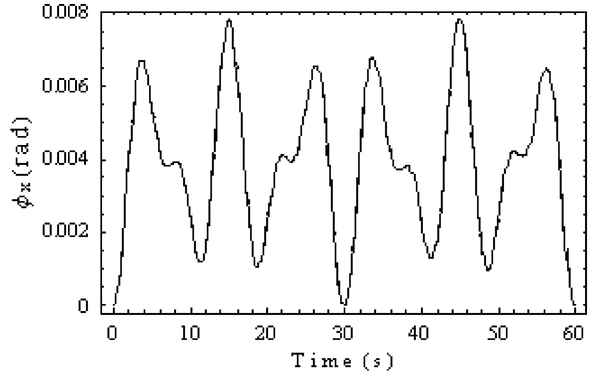

Fig. 4 Exact and analytical solutions for Euler angle ϕ_x.

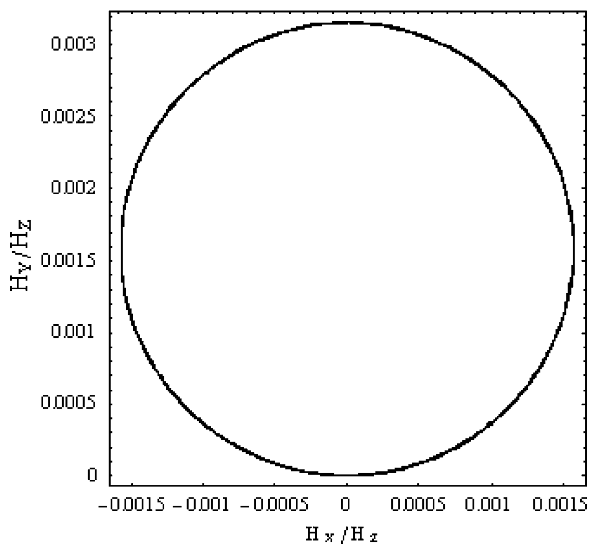

Fig. 5 Exact and analytical solutions for angular momentum pointing.

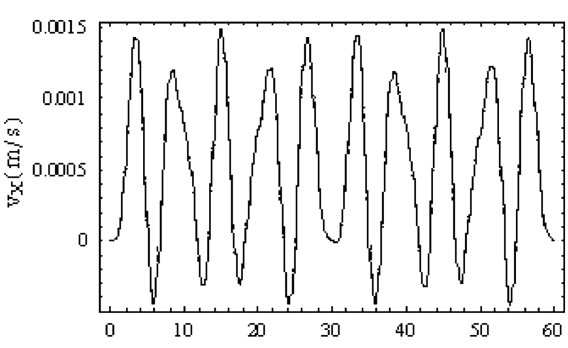

Fig. 6 Exact and analytical solutions for inertial velocity v_X.

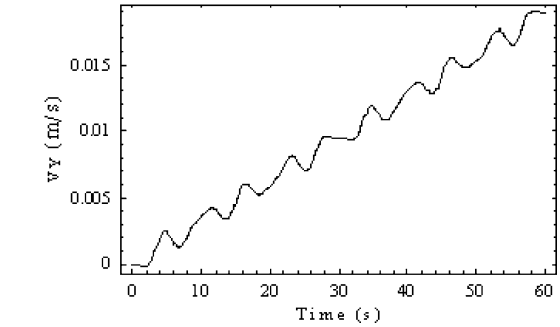

Fig. 7 Exact and analytical solutions for inertial velocity v_Y.

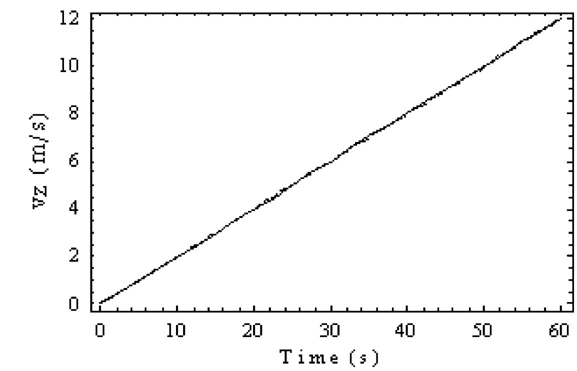

Fig. 8 Exact and analytical solutions for inertial velocity v_Z.

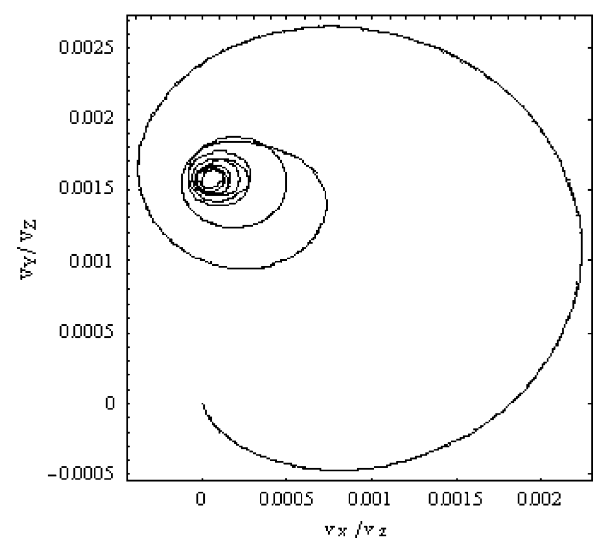

Fig. 9 Exact and analytical solutions for velocity pointing.

it grows with time, the error is of the order 10^{-7} rad/s after 60 s. [The solution for $\omega_y(t)$ is similar, and so we do not present its plot.]

In Fig. 4, we plot the exact solution (solid) and the analytical solution (dashed) for the Euler angle $\phi_x(t)$ obtained from the real part of Eq. (25). [The solution for $\phi_y(t)$ is similar, and so we do not show it.] The difference in the two solutions for ϕ_x (and ϕ_y, which is not shown) is indistinguishable. The error in the analytical solution of $\phi_x(t)$ and $\phi_y(t)$ grows to about 10^{-6} rad after 60 s.

Figure 5 shows the exact (solid) and analytical (dashed) solutions for the pointing of the angular momentum vector, which is indistinguishable in the plot. We note that the trajectory of the tip of the angular momentum vector is a circle with a center at $\left(-M_y/I_z\omega_{z0}^2, M_x/I_z\omega_{z0}^2\right)$ or (0, 1.6 mrad). These numerical results are consistent with the analytical theory.

Figures 6–8 show the exact (solid) and analytical (dashed) solutions for the inertial components of transverse velocity, namely, v_X, v_Y, and v_Z. The analytical solutions are obtained from the real and imaginary parts of Eq. (51) and from Eq. (61). The errors grow to order 10^{-7} m/s for both transverse components and to 10^{-4} for the axial component after 60 s. The behavior of the transverse velocity components is predicted by the secular velocity ratios given in Eqs. (67) and (68). Because $M_y = 0$, Eq. (67) predicts that in the limit as $t \to \infty$, $(v_{X\,\mathrm{sec}}/v_{Z\,\mathrm{sec}}) \to 0$. Thus we see in Fig. 6 that v_X is bounded, whereas in Fig. 8 v_Z grows linearly with time. However, because $M_x \neq 0$, Eq. (68) indicates that the velocity pointing error is not zero. We see in Fig. 7 that v_Y grows linearly with time just as v_Z does. Again, this behavior is as expected from illustration in Fig. 1, where we have growing components of the velocity along the Y and Z inertial directions but not along the X inertial direction. (Of course, if $M_y \neq 0$, then we would see a secular term in v_X.)

Figure 9 plots the velocity pointing in inertial space (v_Y/v_Z, v_X/v_Z). Here we see that the velocity asymptotically approaches the direction of the average path of the angular momentum vector

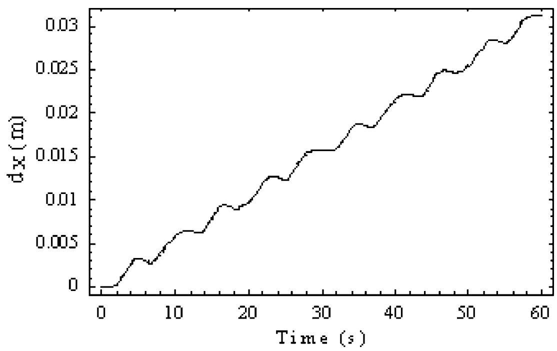

Fig. 10 Exact and analytic solutions for inertial displacement d_X.

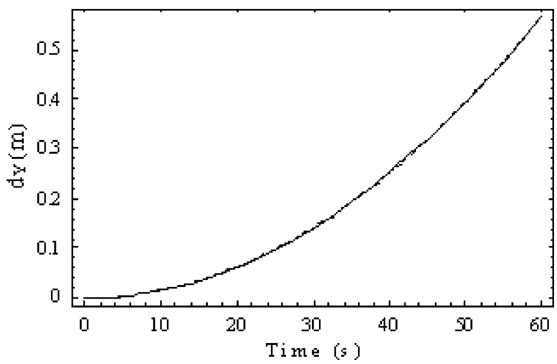

Fig. 11 Exact and analytical solutions for inertial displacement d_Y.

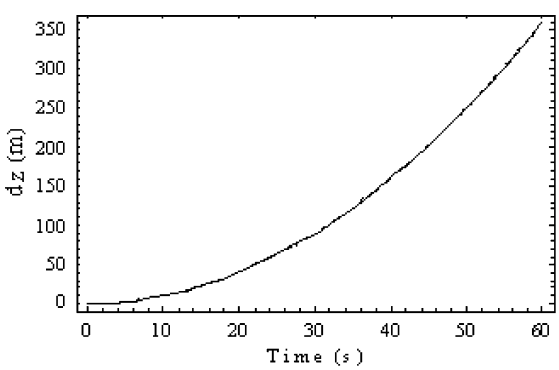

Fig. 12 Exact and analytical solutions for inertial displacement d_Z.

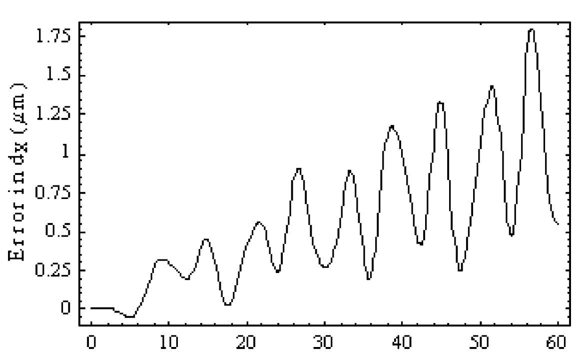

Fig. 13 Exact minus analytical solution of inertial displacement d_X.

centered at (0, 1.6 mrad). We refer the interested reader to Ref. 34 for more details.

Figures 10–12 show the exact (solid) and analytical (dashed) solutions for the inertial components of transverse and axial displacements, namely, d_X, d_Y, and d_Z. (By inertial displacement we mean displacement with respect to an inertial frame originally traveling with the spacecraft before the thruster burn.) The analytical solutions are obtained from the real and imaginary parts of Eq. (57) and Eq. (70). Figure 12 exhibits parabolic growth with time for d_Z, as we expect. The error (shown in Fig. 13) grows to the order 10^{-6} m.

Conclusions

We have presented some generic approximate closed-form solutions for the thrusting, spinning spacecraft problem under the assumptions of constant transverse torques, zero axial torque, and nearly axisymmetric body. Compact analytical solutions are given in complex form for Euler angles, angular momentum, inertial velocities, and displacements. Numerical integration of (and comparison with) the original exact differential equations reveals that the closed-form solutions are highly accurate and eminently applicable to typical spin-stabilized rockets and spacecraft. This work provides an enhanced theoretical understanding of fundamental rigid-body dynamics and a basis for future work and more sophisticated theories. The original solutions can serve as the groundwork for computational algorithms that provide the attitude, rotational, and translational state of the body at any time, allowing parametric studies in rocket, missile, and spacecraft design. These closed-form solutions also have potential applications in onboard (autonomous) computations of spacecraft maneuvers, where speed, accuracy, and memory place severe constraints on numerical algorithms.

References

[1]Cochran, J. E., "Effects of Gravity-Gradient Torque on the Rotational Motion of a Triaxial Satellite in a Precessing Elliptic Orbit," *Celestial Mechanics and Dynamical Astronomy*, Vol. 6, No. 2, 1972, pp. 127–150.

[2]Kraige, L. G., and Junkins, J. L., "Perturbation Formulations for Satellite Attitude Dynamics," *Celestial Mechanics and Dynamical Astronomy*, Vol. 13, No. 1, 1976, pp. 39–64.

[3]Kraige, L. G., and Skaar, S. B., "A Variation of Parameters Approach to the Arbitrary Torqued, Asymmetric Rigid Body Problem," *Journal of the Astronautical Sciences*, Vol. 25, No. 3, 1977, pp. 207–226.

[4]Cochran, J. E., and Shu, P. H., "Attitude Motion of Spacecraft with Skewed Internal Angular Momenta," *Journal of the Astronautical Sciences*, Vol. 31, No. 2, 1983, pp. 203–215.

[5]Kane, T. R., and Levinson, D. A., "Approximate Description of Attitude Motions of a Torque-Free, Nearly Axisymmetric Rigid Body," *Journal of the Astronautical Sciences*, Vol. 35, No. 4, 1987, pp. 435–446.

[6]Junkins, J. L., Jacobson, I. D., and Blanton, J. N., "A Nonlinear Oscillator Analog of Rigid Body Dynamics," *Celestial Mechanics and Dynamical Astronomy*, Vol. 7, No. 4, 1973, pp. 398–407.

[7]Morton, H. S., Junkins, J. L., and Blanton, J. N., "Analytical Solutions for Euler Parameters," *Celestial Mechanics and Dynamical Astronomy*, Vol. 10, No. 4, 1974, pp. 287–301.

[8]Likins, P. W., "Attitude Stability Criteria for Dual-Spin Spacecraft," *Journal of Spacecraft and Rockets*, Vol. 4, No. 12, 1967, pp. 1638–1643.

[9]Larson, V., and Likins, P. W., "Fuel-Optimal Angular Momentum Vector Control for Spinning and Dual-Spin Spacecraft," *Acta Astronautica*, Vol. 18, No. 3, 1973, pp. 215–227.

[10]Junkins, J. L., and Turner, J. D., "Optimal Continuous Torque Attitude Manoeuvres," *Journal of Guidance, Control, and Dynamics*, Vol. 3, No. 4, 1980, pp. 210–217.

[11]Winfree, P. K., and Cochran, J. E., "Nonlinear Attitude Motion of a Dual-Spin Spacecraft Containing Spherical Dampers," *Journal of Guidance, Control, and Dynamics*, Vol. 9, No. 4, 1986, pp. 681–690.

[12]Larson, V., and Likins, P. W., "Closed-Form Solutions for the State Equation for Dual-Spin and Spinning Spacecraft," *Journal of the Astronautical Sciences*, Vol. 21, No. 5–6, 1974, pp. 244–251.

[13]Cochran, J. E., and Shu, P. H., "Attitude Motion of Asymmetric Dual-Spin Spacecraft," *Journal of Guidance, Control, and Dynamics*, Vol. 5, No. 1, 1982, pp. 37–42.

[14]Bödewadt, U. T., "Der Symmetrische Kreisel bei Zeitfester Drehkraft," *Mathematische Zeitschrift,* Vol. 55, 1952, pp. 310–320.

[15]Leimanis, E., *The General Problem of the Motion of Coupled Rigid Bodies About a Fixed Point*, Springer-Verlag, New York, 1965, Chap. 2.

[16]Longuski, J. M., "On the Attitude Motion of a Self-Excited Rigid Body," *Journal of the Astronautical Sciences*, Vol. 32, No. 4, 1984, pp. 463–473.

[17]Longuski, J. M, "Solution of Euler's Equations of Motion and Eulerian Angles for Near-Symmetric Rigid Bodies Subject to Constant Moments," AIAA Paper 80-1642, Aug. 1980.

[18]Longuski, J. M., "Real Solutions for the Attitude Motion of a Self-Excited Rigid Body," *Acta Astronautica*, Vol. 25, No. 3, 1991, pp. 131–140.

[19]Longuski, J. M., Kia, T., and Breckenridge, W. G., "Annihilation of Angular Momentum Bias During Spinning-Up and Thrusting Maneuvers," *Journal of the Astronautical Sciences*, Vol. 37, No. 4, 1989, pp. 433–450.

[20]Price, J. L., "An Economical Series Solution of Euler's Equations of Motion, with Application to Space-Probe Maneuvers," American Astronautical Society, Paper 81-105, Aug. 1995.

[21]Van der Ha, J. F., "Perturbation Solution of Attitude Motion Under Body-Fixed Torques," *Acta Astronautica*, Vol. 12, No. 10, 1985, pp. 861–869.

[22]Rosser, J. B., Newton, R. R., and Gross, G. L., *Mathematical Theory of Rocket Flight*, McGraw–Hill , New York, 1947, pp. 49–262.

[23]Davis, L., Jr., Follin, J. W., Jr., and Blitzer, L., *Exterior Ballistics of Rockets*, Van Nostrand, Princeton, NJ, 1958, Chap. 9.

[24]Armstrong, R. S., "Errors Associated with Spinning-Up and Thrusting Symmetric Rigid Bodies," Jet Propulsion Lab., California Inst. of Technology, Technical Rept. 32-644, Pasadena, CA, Feb. 1965.

[25]Longuski, J. M., "Galileo Maneuver Analysis," American Astronautical Society, Paper 81-137, Aug. 1981.

[26]Longuski, J. M., Campbell, R. S., and Klumpe, E. W., "Error Analysis for Pulsed Maneuvers of a Dual-Spin Spacecraft," AAS/AIAA Astrodynamics Specialist Conf., AAS Paper 89-396, Aug. 1989.

[27]Tsiotras, P., and Longuski, J. M., "A Complex Analytical Solution for the Attitude Motion of a Near-Symmetric Rigid Body Under Body-Fixed Torques," *Celestial Mechanics and Dynamical Astronomy*, Vol. 51, No. 3, 1991, pp. 281–301.

[28]Klumpe, E. W., and Longuski, J. M., "Secular Solution for Delta-V During Spin Rate Change Maneuvers of Rigid Body Spacecraft," AIAA Paper 84-2011, Aug. 1984.

[29]Beck, R. A., and Longuski, J. M., "Analytical Solution for the Velocity of a Rigid Body During Spinning-Up Maneuvers," AIAA Paper 94-3713, Aug. 1994.

[30]Randall, L. A., Longuski, J. M., and Beck, R. A., "Complex Analytic Solutions for a Spinning Rigid Body Subject to Constant Transverse Torques," American Astronautical Society, Paper 95-373, Aug. 1995.

[31]Greenwood, D. T., *Principles of Dynamics*, 2nd ed., Prentice–Hall, Englewood Cliffs, NJ, 1988, p. 392.

[32]Wertz, J. R. (ed.), *Spacecraft Attitude Determination and Control*, D. Reidel, Dordrecht, The Netherlands, 2000, pp. 760–766.

[33]Gick, R. A., "Analysis of the Motion of Spinning, Thrusting Spacecraft," Ph.D. Dissertation, School of Aeronautics and Astronautics, Purdue Univ., West Lafayette, IN, 1999, pp. 17, 18.

[34]Javorsek, D., II, and Longuski, J. M., "Velocity Pointing Errors Associated with Spinning Thrusting Spacecraft," *Journal of Spacecraft and Rockets*, Vol. 37, No. 3, 2000, pp. 359–365.